

RSC Advances



This is an *Accepted Manuscript*, which has been through the Royal Society of Chemistry peer review process and has been accepted for publication.

Accepted Manuscripts are published online shortly after acceptance, before technical editing, formatting and proof reading. Using this free service, authors can make their results available to the community, in citable form, before we publish the edited article. This *Accepted Manuscript* will be replaced by the edited, formatted and paginated article as soon as this is available.

You can find more information about *Accepted Manuscripts* in the [Information for Authors](#).

Please note that technical editing may introduce minor changes to the text and/or graphics, which may alter content. The journal's standard [Terms & Conditions](#) and the [Ethical guidelines](#) still apply. In no event shall the Royal Society of Chemistry be held responsible for any errors or omissions in this *Accepted Manuscript* or any consequences arising from the use of any information it contains.

Energy harvesting from humidity changes with a flexible coaxial electrode solid-state cell

Jesse Smithyman*, Richard Liang

High-Performance Materials Institute, Florida State University, 2005 Levy Ave, Tallahassee, FL 32310, USA

jessesmithyman@gmail.com, liang@eng.fsu.edu

Abstract

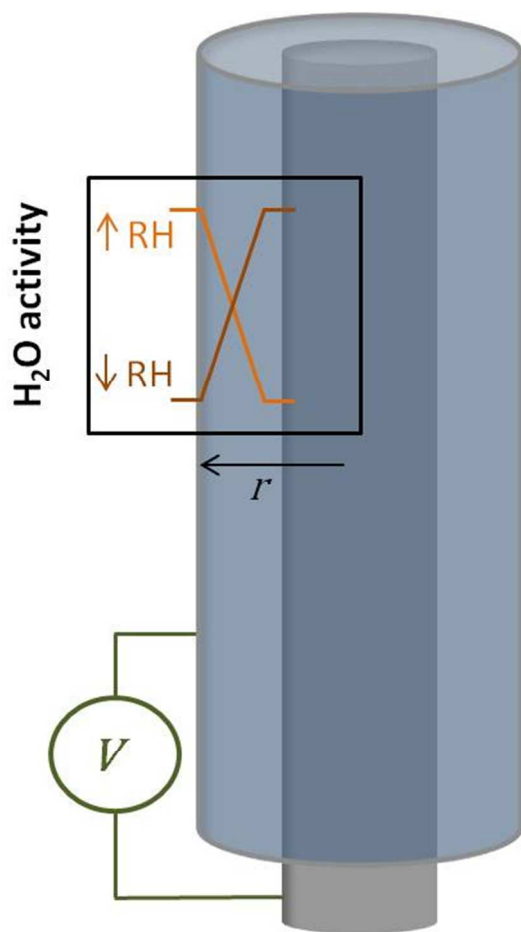
The response to humidity changes from the open-circuit potential (OCP) of a coaxial electrode polymer electrolyte cell was characterized. The OCP response showed a dependency on both the rate of change of the humidity and on the rate of water diffusion within the electrolyte, suggesting the Gibbs free energy due to ionic concentration gradients as the source of the OCP response. This is supported through the estimation of the membrane potential using the Nernst equation and the good agreement between the experimental and theoretical results. The method exploits the hygroscopic properties of the polymer electrolyte and utilizes changes in the relative humidity (RH) of the surrounding environment to induce a concentration gradient between the electrodes. The establishment of the concentration gradient is achieved through the use of a solid-state electrochemical cell with a coaxial electrode structure, enabling the exposure of only one of the electrodes to the environment. These results have implications for applications such as energy harvesting and self-powered sensors and additionally may provide a novel approach to studying the thermodynamic properties of polymer electrolytes.

Keywords

Humidity, solid-state, carbon nanotube, potentiometric, Gibbs free energy

*Corresponding author: Jesse Smithyman, jrs03n@my.fsu.edu, 1-954-547-3081

Graphical Abstract



Introduction

The ability to obtain a potential difference across membranes separating two aqueous solutions of differing salt concentrations has been known for over half a century¹. After Pattle's "hydroelectric pile" in 1954, several approaches have been discussed to extract this Gibbs free energy present in salinity differences for energy harvesting^{2 3 4}. In this report, we present a novel approach to the extraction of this free energy of mixing using a solid-state electrochemical cell and changes in the relative humidity of the surrounding environment. The traditional electrochemical methods contain an essentially fixed volume of water and establish the salinity differences by changing the salt concentration within this volume (*e.g.* compartmentalizing or alternating the flow between fresh and salt water). Conversely, we have observed a potential difference across a polymer electrolyte that contains essentially fixed ions, where the concentration gradient is established due to an increase or decrease in the local water content of the outer electrode.

This local concentration change occurs due to the hygroscopic nature of the polymer electrolyte and its ability to rapidly exchange H₂O molecules with the surrounding environment as the relative humidity changes. The occurrence of this absorption/desorption at only one of the electrodes is critical to the establishment of the concentration gradient and is achieved through the use of a coaxial electrode cell architecture. The coaxial architecture ensures that the inner electrode is shielded from the surrounding environment, thereby causing the water absorption/desorption to occur only at the outer electrode.

Experimental

Equipment and data acquisition

A controlled environment chamber from Electro-Tech Systems, Inc. was used to regulate the humidity via an ultrasonic humidifier and desiccant/pump dehumidification system and PID controller. The data from the chamber humidity sensor (capacitive film type) and the coaxial cell were simultaneously recorded using a custom LabView program (LabView 2009 SP1, Version 9.0.1f3). The OCP was measured using a nanovoltmeter from Keithley Instruments (Model 2182A) and connected to the computer (HP Presario CQ56 Notebook PC, 64-bit Windows 7) using a GPIB controller for hi-speed USB from National Instruments Corporation. The data acquisition rate of the LabView program was 1 point per second. A VersaSTAT3 with

Frequency Response Analyzer upgrade from Princeton Applied Research was used in Zero Resistance Ammeter mode to measure the short-circuit current of the cell.

Materials and fabrication process

Carbon nanotube yarn (CTex™) and non-woven CNT sheets were purchased from Nanocomp Technologies, Inc., and were used as received. Nafion 117 solution and lithium hydroxide monohydrate (98%) were purchased from Sigma-Aldrich. The inner electrode was constructed by twisting multiple filaments of CNT yarn (length ~ 10 cm) together. The inner electrode was then coated with lithium exchanged Nafion (Li-Nafion) by several iterations of dip coating in Li-Nafion solution followed by annealing for 6 hours at 120 °C after each coating. The Li-Nafion was prepared by adding a 0.5 M LiOH drop-wise to the Nafion 117 solution, while stirring, until the pH reached ~ 8. The outer electrode was applied by hand wrapping multiple layers of thin CNT sheets (~ 1 micron thickness) around the Li-Nafion coated region. The final cell had a maximum diameter of less than 1 mm. SEM images of similar coaxial electrode cells are can be viewed in our previous report on flexible electrochemical double-layer capacitors ⁵.

Results and Discussion

Changes in the humidity induced action potential-like response waveforms in the cell OCP where, after reaching a peak potential would decrease and undershoot the initial OCP before slowly returning towards the resting potential. These action potential-like responses are shown in Figure 1 overlaid with the data from the chamber's commercial humidity sensor for a 10% increase and 10% decrease in humidity.

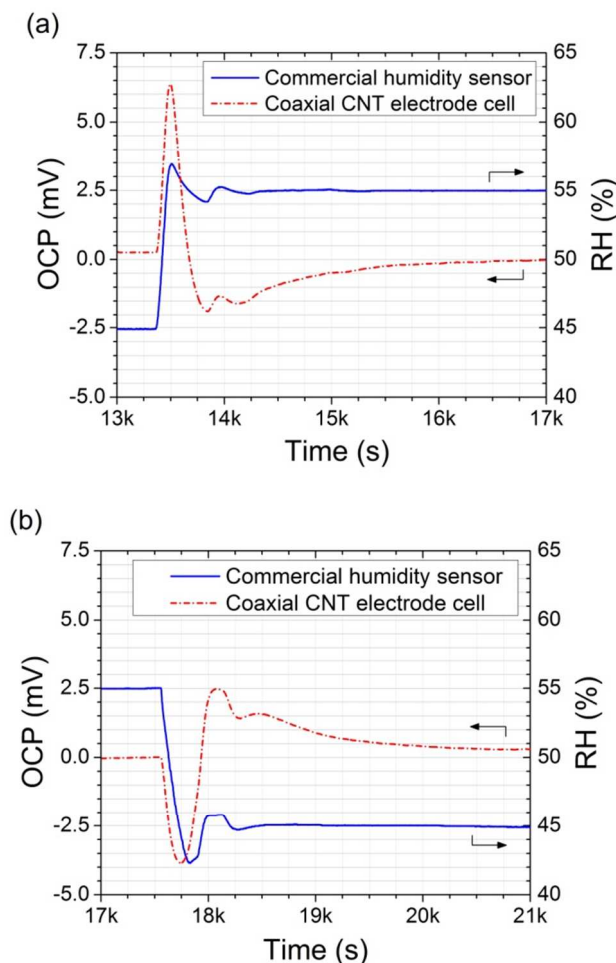


Figure 1. Data from a commercial humidity sensor overlaid with the open-circuit potential (OCP) of coaxial CNT electrode cell for (a) 10% step-change in the RH from 45% to 55% and (b) 10% decrease from 55% to 45%.

Unlike the rapid action potentials of excitable animal cells which contain non-responsive refractory periods, the OCP of the coaxial cell was still responsive to humidity changes during its slow return towards the resting potential. This is demonstrated by the oscillations in the RH prior to its stabilization at the target humidity due to the PID control mechanism used for its regulation. These oscillations produce peaks in the RH that are also captured by the OCP during its return to equilibrium for both an increase or decrease in humidity, as shown in Figure 1a and Figure 1b.

The repeatability of the OCP response was investigated by performing three iterations of a 10% increase, 10% decrease cycling of the RH at three different humidity levels: 35% - 45%, 45%-55% and 55% - 65%. Following each step change, the humidity was kept constant for at least 1 hour to allow the cell's OCP to return to a quasi-equilibrium/resting potential prior to

each humidity step change. Figure 1 is provided as a representative sample of the results from the cycling tests. The original data for all tests are provided in the Supplementary Information.

The coordinates (x, y) of both the RH and OCP peaks were obtained using the Peak Analyzer function in the OriginLab software program. Two quantities were calculated from the peak data in order to compare the data sets and analyze the characteristics of the OCP response. The first is a calculation of the time difference between the RH peak and the corresponding OCP peak to quantify the lag between the data sets. The calculation of the time between peaks (Δt) is defined here as the time (*i.e.* x-coordinate) of the OCP peak (t_{OCP}) subtracted from the RH peak (t_{RH}) peak time, as shown in Eqn. (1):

$$\Delta t = t_{RH} - t_{OCP} \quad (1)$$

The second quantity calculated from the peak data is the magnitude (absolute value) of the OCP response. The peak magnitude, or change in the OCP (ΔOCP), is the absolute value of the difference between the peak potential (OCP_{peak}) and the potential prior to the humidity change ($OCP_{initial}$), as shown in Eqn. (2):

$$\Delta OCP = OCP_{peak} - OCP_{initial} \quad (2)$$

A thermodynamic estimate of the potential generated from the humidity induced salinity difference can be calculated through the use of the Nernst relationship as shown in Eqn. (3):

$$\Delta V = \frac{RT}{zF} \ln \frac{a_{H_2O}^{OE}}{a_{H_2O}^{IE}} \quad (3)$$

where ΔV is the theoretical membrane potential ($J C^{-1}$ or V), R is the gas constant ($J mol^{-1} K^{-1}$), T is the absolute temperature (K), z is the electrochemical valence, F is Faraday's constant ($C mol^{-1}$), and $a_{H_2O}^{OE}$ and $a_{H_2O}^{IE}$ are the water activities at the outer and inner electrodes, respectively. The water activity at each electrode can be represented through the humidity data to provide a theoretical prediction of the potential based purely on the thermodynamics of the Gibbs free energy of the salinity difference generated from an increase or decrease of the water activity at an electrode. It should be noted that Eqn. 3 corresponds to a polarity where the inner electrode is positive and could be written alternatively as the negative of the current form for the alternate polarity.

Since the system was allowed to reach equilibrium prior to each test, the initial humidity will provide an accurate representation of the water activity at the inner electrode up until the point when water diffusion to/from the outer electrode reaches the inner electrode and

increases/decreases the local water concentration. To estimate the peak potential induced by the humidity change, the water activity at the outer electrode can be represented by the peak humidity. The thermodynamic prediction of ΔOCP based on the Nernst relationship is shown in Eqn. (4) with the results plotted along with the ΔOCP data in Figure 2.

$$\Delta OCP_N = \frac{RT}{zF} \ln \frac{\text{peak humidity}}{\text{initial humidity}} \quad (4)$$

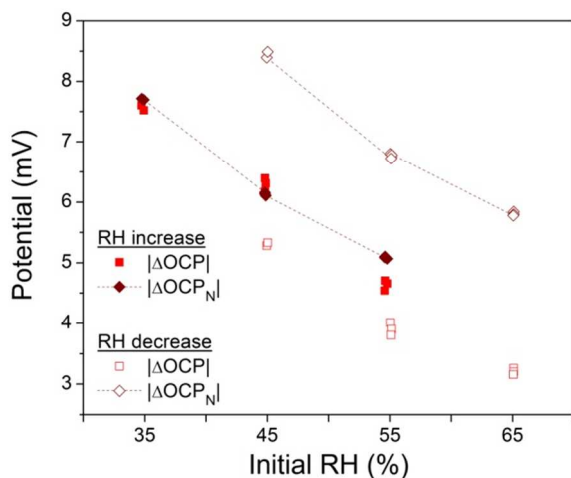


Figure 2. ΔOCP and ΔOCP_N for the first peak of each of the three increase and three decrease events performed at each humidity range: 35% - 45%, 45%-55% and 55% - 65%. The magnitude of the change in RH was the same for all tests ($\sim \pm 12.5\%$).

Figure 2 shows the accuracy of the Nernst equation and is strong supporting evidence of the underlying mechanism of the Gibbs free energy being responsible for the OCP response. In fact, Eqn. (4) can be generalized to calculate the humidity at time i , by replacing the ‘peak humidity’ with the humidity at time i and is highly accurate during conditions of minimal kinetic effects (*i.e.* before diffusion of water reaches the inner electrode). An example for both an increase and decrease in humidity are shown in the Supplementary Information (Figures S12 and S13, Eqn. S1).

First, we can see from Figure 2 that the trend of decreasing ΔOCP with increasing initial RH is a thermodynamic feature of the system under these conditions. Interestingly, the thermodynamic predictions were nearly identical to the peak potentials observed experimentally for the increasing humidity cases, yet a consistent deviation was observed between the experimental and predicted response for the decreasing humidity tests. As seen in Figure 2, according to Eqn. (4), the potentials should be higher for decreasing humidity than the peak

potentials of the increasing humidity tests. In general, deviations from the thermodynamic predictions are likely to occur due to kinetic effects from the properties of the Nafion electrolyte or due to effects of the test conditions. We believe the later is a possible cause for the consistent deviation observed in the decreasing humidity tests. The chamber decreases the humidity by pumping the chamber air through a desiccant column, which typically results in a slower rate of change of the humidity when compared with the increase of humidity from injection of water vapor from an ultrasonic humidifier. The plots of the first derivative of the humidity data are provided in the Supplementary Information for one cycle from each humidity range and show the consistently slower rate of the RH decrease versus the RH increase. While further studies are required to fully elucidate the effects of various kinetic relationships, some insight can be obtained from the results of the time between peaks (Δt) plotted in Figure 3.

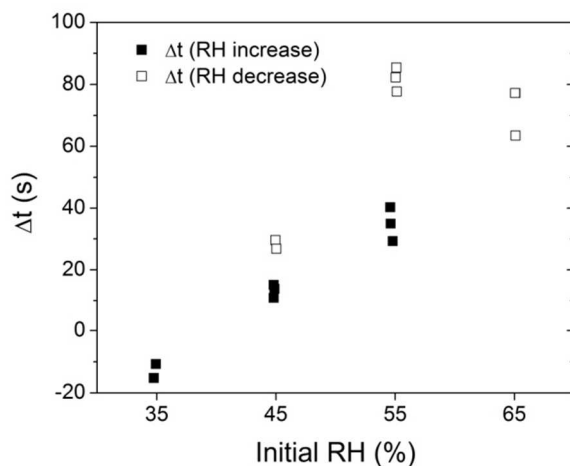


Figure 3. Δt for the initial peaks of each step change. Three increase-decrease cycles were performed at each humidity range: 35% - 45%, 45%-55% and 55% - 65%. The magnitude of the change in RH was the same for all tests ($\sim \pm 12.5\%$).

Figure 3 shows a strong dependency of Δt on the initial humidity with an additional dependency on whether an increase or decrease in RH occurred from that initial RH. With higher initial humidity of the test, a larger Δt is observed, while when starting from the same initial RH, a decrease in humidity always produced a larger Δt than an increase of similar magnitude (all results in Figure 2 and Figure 3 are of the same magnitude change). Note that a positive Δt indicates that the OCP peak *preceded* the RH peak. This preceding peak, or negative lag, of the OCP versus the RH is observable in the original test data shown in Figure 1b for a 55% to 45% decrease event. Such a response would not be expected under the assumption that the OCP is

changing *in response* to the humidity change. The transport properties of the Nafion electrolyte may provide some explanation for these observations.

Dr. Benziger group has shown three important characteristics of water transport through Nafion membranes: 1) the limiting water self-diffusivity in Nafion increases exponentially with water activity ⁶, 2) water desorption is faster than absorption ⁷, and 3) water transport is diffusion limited at lower water concentrations, while at high water content the interfacial transport at the membrane/vapor interface becomes the limiting step. Due to the significant increase in water diffusivity with membrane water content, water diffusion to/from the interface is faster during desorption than adsorption.

Immediately upon establishment of the concentration gradient, water diffusion towards regions of lower water content begins in order to minimize the energy of the system. So long as this diffusion has not changed the local concentration at the inner electrode, and absorption/evaporation continues at the outer electrode, the concentration gradient will continue to increase. However, once the diffusion front reaches the inner electrode, the magnitude of the concentration difference begins to decrease, along with the potential difference observed between the electrodes (*i.e.* causing a peak in the OCP). This would result in the OCP peaking prior to the RH when conditions are such that the rate of the water transport through the electrolyte is limited by interfacial transport (as opposed to diffusion) and the RH step-change is large. Faster diffusion of water will result in the OCP peaking sooner (*i.e.* larger Δt).

On multiple occasions during long periods of constant RH, the humidity displayed a series of low-magnitude ($\sim \pm 0.25$ % RH) oscillations around the humidity set point over a period of 2 ~ 3 hours. The top plot of Figure 4 shows the OCP and RH data during one such period of low-magnitude oscillations in the RH with the first derivatives of each data set shown in the bottom plot.

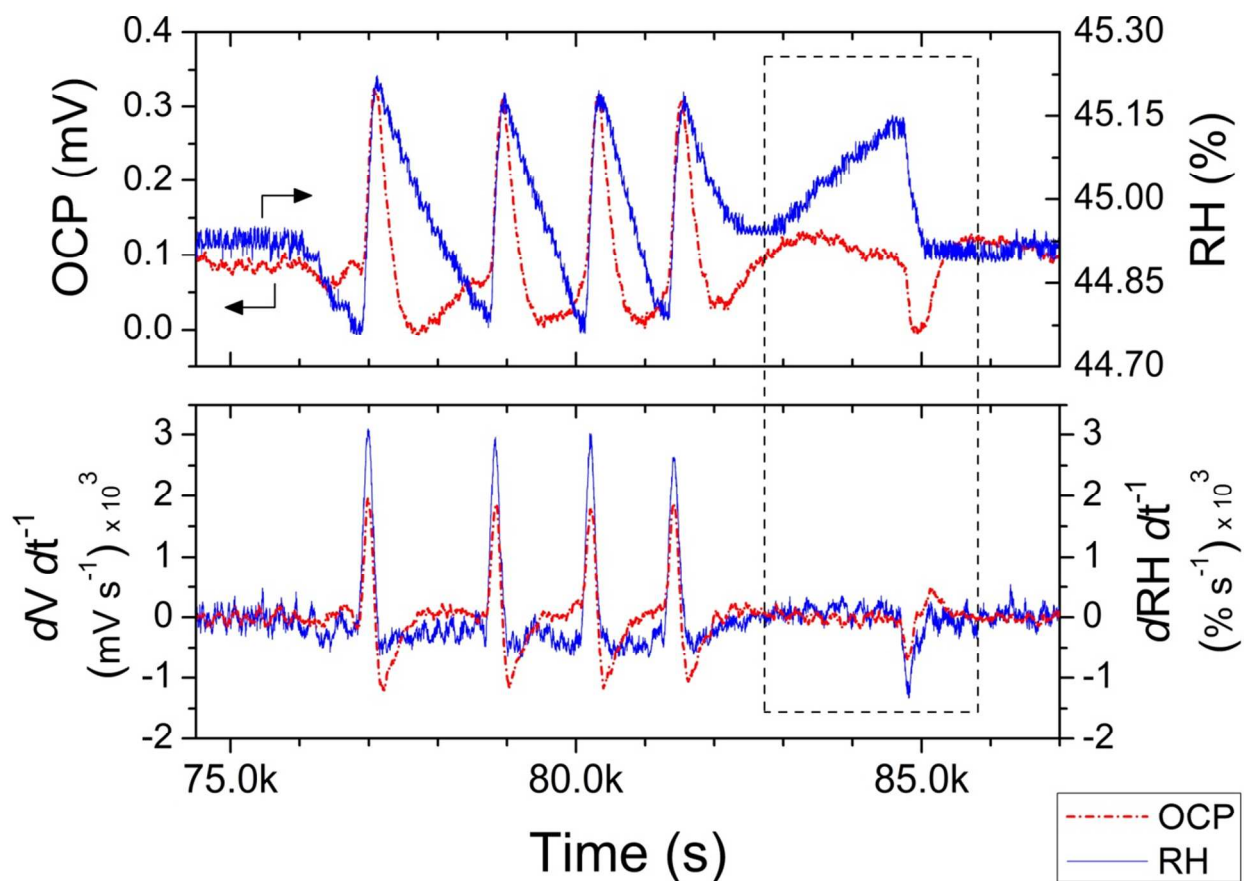


Figure 4. OCP and RH data during a series of low-magnitude humidity changes plotted along with the first derivatives of each. The data outlined in the dashed line provides indication that the underlying mechanism OCP change is dependent on the rate of change of the humidity.

After responding to four consecutive peaks in the RH, the OCP showed no corresponding response to a fifth RH peak. The OCP did however respond to the decrease from the fifth peak as the humidity returned to the RH set point; a response that had not occurred previously for the other declines in RH from the first four peaks. The strong correlation between the first derivatives of the OCP and RH in bottom plot of Figure 4 provides the explanations for these “inconsistencies”. The OCP change is dependent on the *rate of change* of the humidity and not the magnitude of the humidity in and of itself. The gradual increase of humidity to the fifth peak produced no significant peaks in the $dRH dt^{-1}$ as the first four peaks did. However, the decrease from this peak was rapid enough, as observed by the $dRH dt^{-1}$ peak just before the 85k mark, that a corresponding decrease in the OCP occurred.

This dependency on the rate of RH change is in line with the proposed mechanisms responsible for the OCP response. The rate of the humidity change will determine the rate of change in the water content at the outer electrode. If this rate is too slow, and the rate of diffusion through the electrolyte is sufficiently high, then the extent of any concentration gradient, and resulting open-circuit potential, will be minimal to non-existent.

The magnitude of the OCP response to the low-magnitude RH changes was also accurately predicted using the Nernst relationship of Eqn. (4). Figure 5 plots both ΔOCP and ΔOCP_N for the five OCP peaks (four increases and one decrease) from Figure 4.

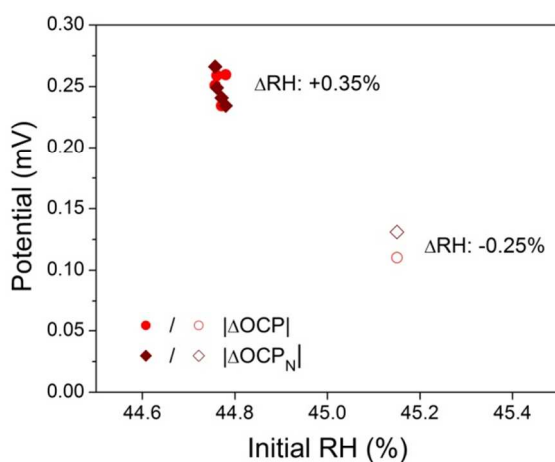


Figure 5. Experimental values of the peak potential (ΔOCP) induced from low-magnitude RH changes ($\sim \pm 0.25\%$) along with the thermodynamic predictions (ΔOCP_N).

The actual extraction or harvesting of this potential energy could occur in a number of ways. While Pattle’s hydroelectric pile drove a direct current, others have utilized the phenomena to

increase the charge stored in batteries or electrochemical capacitors^{3,8,9}. While the cell voltage is governed by the thermodynamics, the current output and resulting power produced are determined by the resistance of the cell^{2,9}. The humidity dependent equivalent series resistance (ESR) the cell is shown in Figure 6. The ESR of electrochemical cells is dominated by the resistance of the electrolyte, and thus shows the strong humidity dependency expected from Nafion¹⁰.

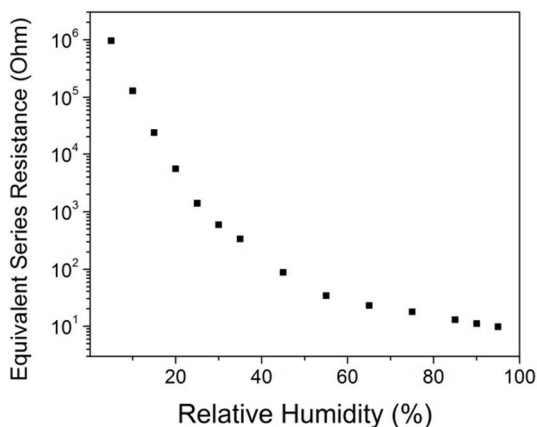


Figure 6. Humidity dependent equivalent series resistance (ESR) of the coaxial cell measured by electrochemical impedance spectroscopy.

The extremely high resistance at low humidity levels would cause significant limitations in the power output and we recommend the use of polymer electrolytes with higher conductivities in low humidity environments to overcome this disadvantage. Nonetheless, we have measured the short-circuit current (I_{sc}) to demonstrate the potential power output of the cell. Figure 6 shows I_{sc} results while cycling the humidity between 35% and 45% RH.

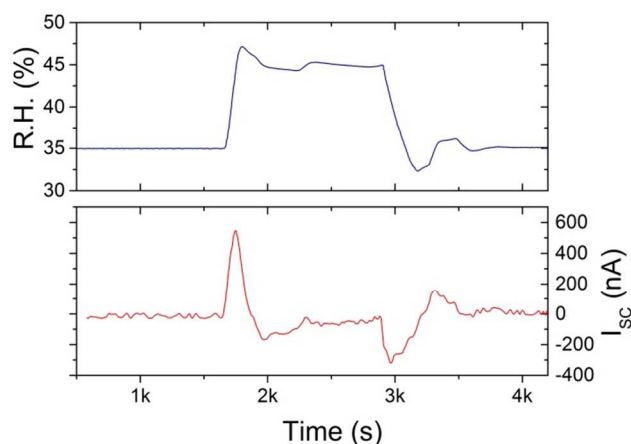


Figure 7. Short-circuit current measured while cycling the humidity between 35% and 45% RH.

Multiplying the peak I_{sc} of ~ 600 nA for the increase from 35% to 45% RH by the peak OCP of ~ 7.5 mV obtained for the same humidity change results in a maximum power of ~ 4 nW. With a cell volume of ~ 0.035 cm³, the peak volumetric power density is ~ 0.13 W m⁻³. The peak I_{sc} increased to ~ 800 nA for the humidity increase from 45% to 55%, showing the effect of the humidity dependent resistance of Nafion (i.e. larger current due to lower cell resistance). However, as previously discussed and illustrated in Figure 2, the OCP decreases as you move into higher RH levels, and thus the results for the maximum power calculation for the 45% to 55% RH increase is only a few tenths of a nanowatt greater than that for the 35% to 45% RH change. This highlights the need to use a polymer electrolyte without the drastic increase in resistance at low humidity levels in order to investigate the limitations of the energy harvesting performance.

Conclusion

We have shown that an open-circuit potential response is generated when a change in the relative humidity occurs in the environment surrounding a solid-state cell composed of coaxial carbon nanotube (CNT) network electrodes and a Nafion polymer electrolyte. The change in humidity will induce a corresponding change in the water content in the Nafion near the outer electrode as water is absorbed or evaporated. The resulting water concentration gradient in the ionic polymer electrolyte between the two electrodes generates a Gibbs free energy that is measurable in the open-circuit potential (OCP) of the cell.

The characteristics of the OCP response will be determined by the difference between the rate of change of the water content at one electrode and that of the opposite electrode. At the

outer electrode, this change rate is determined by the rate of the humidity change, the absorption/evaporation rate and the rate at which water diffuses to/from the electrode. Since the coaxial electrode architecture shields the inner electrode from the surrounding environment, the rate of water diffusion through the electrolyte will determine the rate of change of the water content at inner electrode. Clearly, this inherently dynamic system has many contributing factors, including not only the properties of the electrochemical cell, but also the characteristics of the changing environmental conditions. Further systematic experimental and modeling studies will be required to fully describe the influential factors and the extent of each's impact on the cell's performance. Nonetheless, we have successfully demonstrated the concept, and provided initial studies that should prove useful in guiding future studies.

Just as R.E. Pattle introduced six decades ago with salinity concentration gradients from salt and fresh water, a measurable Gibbs free energy can be obtained from concentration gradients induced in ionic polymers by changes in water content at one electrode. One way to induce such local concentration changes is through changes in the relative humidity of the surrounding environment, and use of a coaxial electrode cell. The established electric potential is governed by the thermodynamics described by the Nernst relationship, and subject to various kinetic effects. The availability of this electrical potential to do work presents the possibility to engineer small, lightweight and flexible devices capable of energy harvesting or providing "self-powered" sensory/detection information. While the data was not shown in this report, we have successfully used a number of different sources to induce the open-circuit potential response, including dry gas flows along with changes in their flow rates, opening and closing of doors, and human breath.

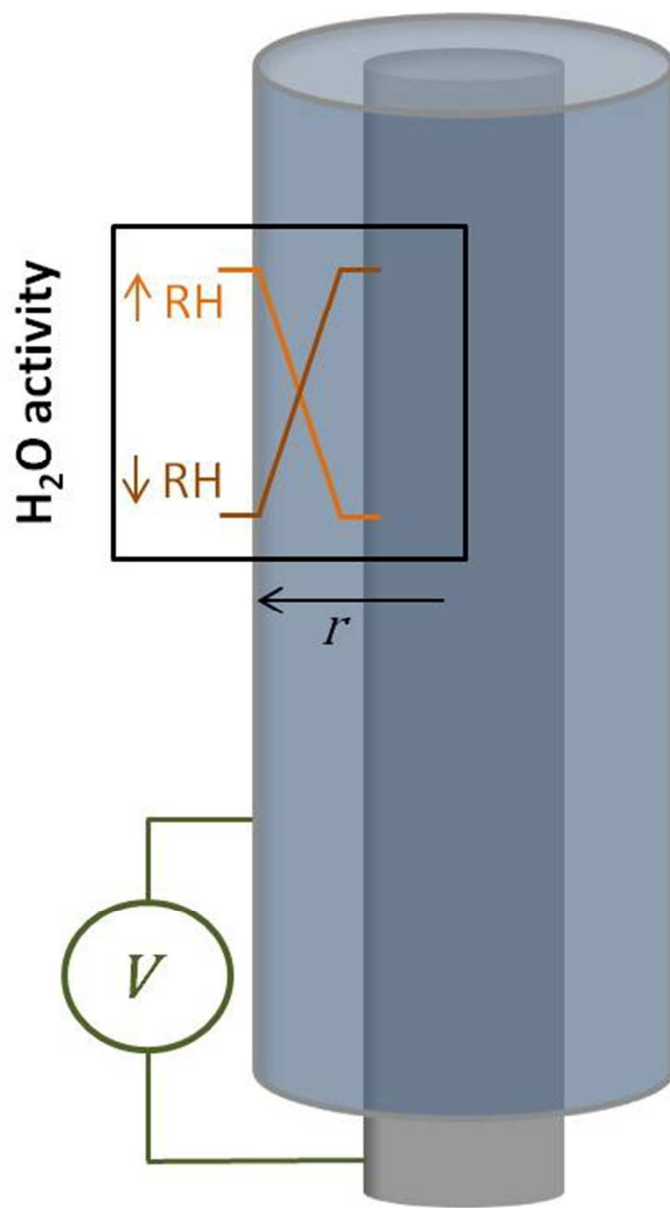
In addition to the attraction for applications, the methods presented may prove useful for studying the fundamental properties of polymer electrolytes and the constituent components of such systems similar. Theoretically, a relatively small and finite amount of water molecules should only be needed (to be absorbed or evaporated) in order to induce a measurable energy change of the system. Such an approach may provide a novel route to perform studies on the solvation or transport properties that is complimentary to the traditional bulk measurement methods used to study these systems.

Acknowledgements

This effort is supported by the High-Performance Materials Institute of Florida State University and the GAP Grant from the Florida State Research Foundation. We would like to thank Dr. JG Park for his help with LabView and equipment interfacing and Dr. Daniel Hallinan for his helpful discussion and insight.

References

1. R. E. Pattle, *Nature*, 1954, 174, 660-660.
2. J.N. Weinstein and F. B. Leitz, *Science*, 1976, 191, 557-559.
3. D. Brogioli, R. Ziano, R. A. Rica, D. Salerno, O. Kozynchenko, H. V. M. Hamelers and F. Mantegazza, *Energy & Environmental Science*, 2012, 5, 9870-9880.
4. M. Olsson, G. L. Wick and J.D. Isaacs, *Science*, 1979, 206, 452-454.
5. J. Smithyman and R. Liang, *Materials Science and Engineering. B*, 2014, 184, 34-43.
6. Q. Zhao, P. Majsztrik and J. Benziger, *The Journal of Physical Chemistry. B*, 2011, 115, 2717-2727.
7. M. B. Satterfield and J. Benziger, *The Journal of Physical Chemistry. B*, 2008, 112, 3693-3704.
8. F. La Mantia, M. Pasta, H. D. Deshazer, B. E. Logan and Y. Cui, *Nano Letters*, 2011, 11, 1810-1813.
9. F. Liu, O. Schaetzle, B. B. Sales, M. Saakes, C. J. N. Buisman and H. V. M. Hamelers, *Energy & Environmental Science*, 2012, 5, 8642-8650.
10. Y. Sone, P. Ekdunge and D. Simonsson, *Journal of the Electrochemical Society*, 1996, 143, 1254-1259.



71x122mm (150 x 150 DPI)